Utilization of the Spectral Density -derived From the Recordings of the Random Defects on a Railway Track- in the Maintenance Works

KONSTANTINOS SP. GIANNAKOS
Civil Engineer, dipl. NTUA, PhD AUTh; Fellow/Life-Member of the Amer. Soc. Civ. Eng. (ASCE)
f. adjunct Professor, University of Thessaly, Civil Engineering Dpt.
Ambassador of WSEAS [= *World Scientific and Engineering Academy and Society]*
108 Neoreion str., Piraeus 18534
GREECE

Abstract: - The present article is a continuation of [21] and [22]; after the examination of the reliability of the recordings of the defects on Track by the Track Recording Cars, it presents real graphs of recordings of some Track parameters, the Spectral Densities for the defects of leveling and examines the Dynamic Vertical Stresses on the Trackbed due to the Excitation Spectra of the Track, the Response of the "Track-Vehicle system" to the Track defects in relation to their Spectral Density, a Statistical Analysis of Spectra of the Track Recordings, as well as the utilization of Spectra to make correct decisions for the Track maintenance works. The real data being presented in the article resulted from theoretical and experimental investigations to which the author participated since the cooperation between experts of Greek and French State Railways (1988-1989) until quite recently (2025).

Key-Words: Excitation, Response, Spectral, Density, Railways, Track, Vehicle, graphs, defects.

Received: March 16, 2025. Revised: August 13, 2025. Accepted: September 15, 2025. Published: December 19, 2025.

1 Introduction

The present article is a continuation of the previous articles: (a) "*Railway System 'Vehicle-Track': Relation Between the Spectral Density of Excitation vs Response*" [21] and (b) "*Railway System 'Vehicle-Track': Simulation, Mathematical Modelling and Spectral Densities of Excitation and Response (Part II)*" [22]. It focuses on the use of Track Recordings in the daily practice -and in theory too- of Track Engineers, in order to make decisions about the works to be performed for the Track maintenance.

Statistics play a significant role in spectral analysis in this case, because most signals have a noisy or random aspect. If the underlying statistical attributes of a signal were known exactly or could be determined without error from a finite interval of the signal, then spectral analysis would be an exact science. Finally, the practical reality documents that -indeed- an estimate of the spectrum can be made from even a single finite segment of an infinite signal [23].

We should remember that [21]: in Railways "the Train circulation is a random dynamic phenomenon and, according to the different frequencies imposed by the loads, and the corresponding response of track superstructure. The dynamic component of the load of the vehicle on the track depends on the mechanical properties (stiffness, damping) of the system "vehicle-track", which acts as an excitation on the vehicle's motion (Figures 4, 9) and, vice-versa, the vehicle's motion acts as an excitation on the track. The most simplified approach of this motion (vehicle on Track) is simulated by a SDOF [= Single Degree of Freedom] system (Figure 9)". [22]

The dynamic component of the acting load is primarily caused by the motion of the vehicle's Non-Suspended (Un-sprung) Masses, which are excited by the track geometry and the vertical defects, and, to a smaller degree, by the effect of the Suspended (sprung) Masses. In order to evaluate the real defects of the Track and their influence on the acting forces we use Track Recording cars whose reliability was presented recently ([21], [22], [[13]).

In order to calculate the magnitude of this dynamic component of the acting Load we use a theoretical analysis based on the Fourier Transforma-

tion, which approaches the phenomenon as the Loads -owed to forced random oscillations in systems with damping-appear. In the following, we will present this procedure. The forms of the excitations are random by nature and not deterministic. [[22]]

2 Recordings of the Track Parameters

During the period 1987–2014, and even later, the author took part in a research program with many stages ([9], [8], [25], [26]). During his participation in the Cooperation OSE/SNCF[1] several matters were examined thoroughly, and the evaluation of the Track Recordings performed by the Track Recording Vehicles -of each network- was one of them.

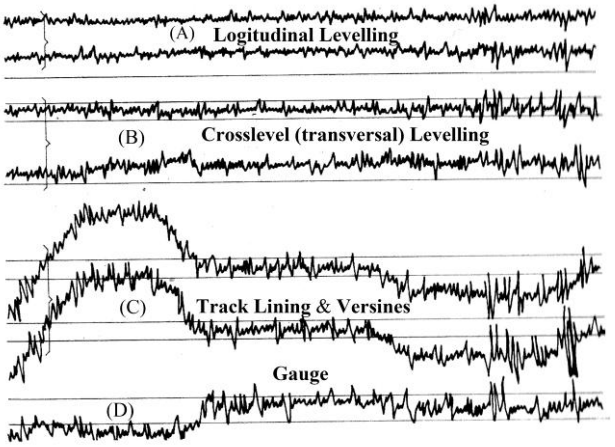

Figure 1. Recordings of some of the parameters of a section of a Track: (A) the levelling along the Track, (B) the levelling in the transverse direction to the Track's axis, the crosslevel, (C) the Track lining (Dressage in French) with the versines' recording of a curve at the left part and, (d) the Gauge of the Track.

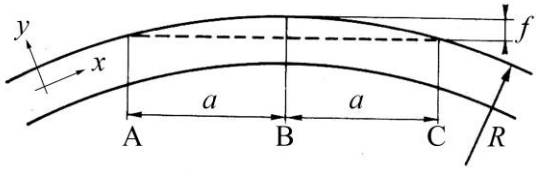

Figure 2. A curve of radius *R*, the axes of the two rails and the measurement of the versine *f* (of the outer rail) in the middle of a chord of *2a* length.

In Fig. 1 the graphs of Track Recordings are presented. They were contributed by the experts of the SNCF during the meetings (Cooperation OSE/SNCF, (see [25], [26]) on 1988-1989 and they are included in [9] (Meetings' Minutes) and [8] (Report of the Experts' Committee of OSE); all of them are presented also in [1]. The translations of the terminology in the English language have been performed, based on the British Permanent Way Institution [4].

The term versine in a curve of radius R is defined in Fig. 2, and its magnitude is given by Eqn. 2.1:

$$f = \frac{a^2}{2 \cdot R} \tag{2.1}$$

The Recording(s) of the levelling (along the Track (a) or in the transversal direction (b) of the axis of the Track (crosslevel)) is/are the fluctuation of the position of the real Rail Running Table/Surface (the contact area of the Rail-head to the wheel, or, the surface where the [bandages of the] wheels roll) *in the vertical axis in space -namely z-*, if *x* represents the direction along the Track and *y* is the transversal direction to the axis of the Track in the same crosslevel (see Fig. 2).

The longitudinal leveling of each rail, obtained by the recording, using a system consisting of a central transducer, the vertical displacement of whose is measured, relatively to the level of the two or four -dependent on whether the Vehicle has axles or two-axle bogies- axles of the Track Recording Vehicle traveling along the same rail. The reference level to which the leveling is related is therefore not perfectly determined; but what matters, in practice, at least for speeds not exceeding 200 km/h, is to know the local leveling differences relative to the average longitudinal profile of the track, calculated on a base corresponding approximately to that of the Recording Car, or elongated in relation to it by using filtering or inertial processes.

All these measurements, except the one referring to the twist (not presented in Fig.1 here) which is doubled, appear in true size on the recordings (which are recorded also in magnetic material) which are recorded at a rate of 20-100 cm per kilometer. The scale is sufficient for one to be able to precisely locate the defects, in relation to the rail joints or rail welds, which often result in clear and distinct low points on both rails.

Further studies on the statistical analysis of the Track-defects have revealed a drawback of these devices: due to their design, recording vehicles distort the measurements of the geometric condition of the tracks [cf. [21], [22]]. While this distortion is generally minor, it plays a fundamental role when analyzing defects by wavelength, as some wavelengths, whether in leveling or alignment,

[1] OSE the initials in Greek of the Organization of Railways in Greece; SNCF the initials of the French National Society of Railways.

disappear completely, as it had been shown in [[30]], [[8]]. Therefore, there is a "transfer function" of the vehicle that must be corrected in the computers performing statistical analysis of the Track defects.

3 Final Position in the z-axis of the Rail Running Surface/Table during the passage of an Axle from a Point x_0

During the circulation of a vehicle on a Railway Track, if we take a time-instant t_0 when an axle passes over a point x_0 then Fig. 3 depicts what happens.

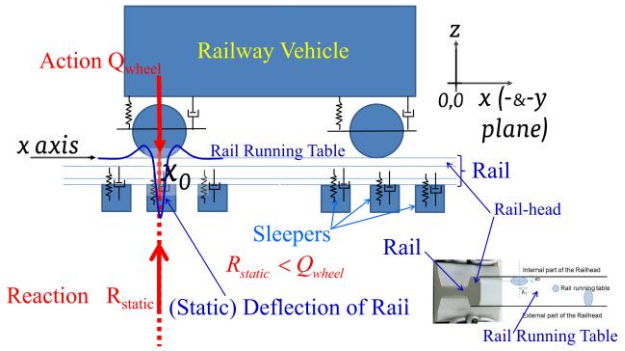

Figure 3. (Upper) A Railway Vehicle on a Track: the axle of the vehicle on the point x_0 (at time-instant t_0) exerts a static load Q_{wheel}; the Reaction $R_{static} < Q_{wheel}$ since, due to the (static) deflection of the rail, the load is distributed to the adjacent sleepers. (Lower at the right of the Figure) A Rail with the Rail-head and the Rail Running Surface on the upper surface of the Rail-head with the ellipses of the contact between Rail-Wheel (see [14]).

Where $\rho_{static\text{-}total}$ is given (Fig. 4upper-lower) by Eqn. (3.2.).

$$\frac{1}{\rho_{total}} = \frac{1}{\rho_{rail}} + \frac{1}{\rho_{pad}} + \frac{1}{\rho_{sleeper}} + \frac{1}{\rho_{ballast}} + \frac{1}{\rho_{substructure}} \quad (3.2)$$

The final position of the Rail Running Table, at point x_0, in the vertical (z-axis) in space, is the sum of five (vertical) component-displacements/subsidence(s):[2]

a.-The deflection y_{static} due to the Q_{static} exerted by the rolling wheel on the Track; the static Load is distributed to the adjacent sleepers thus the Reaction R_{static} on each support-point of the Track < Q_{static}. This static deflection is given by the Eqn. (3.1.) [[17], 307].

$$y_{static} = Q_{total} \cdot \frac{1}{2\sqrt{2}} \cdot \sqrt[4]{\frac{\ell^3}{E \cdot J \cdot \rho_{total}^3}} \quad (3.1)$$

[2] I would like to thank professor T.P. Tassios for his suggestion to clarify this point.

b.-The deflection $y_{dynamic}$ owed to the Dynamic Component of the Load. This component is not distributed to the adjacent sleepers due to the high frequency of the Dynamic Component of the Load and the subsequent inability of the Track to follow (to respond) in these frequencies.

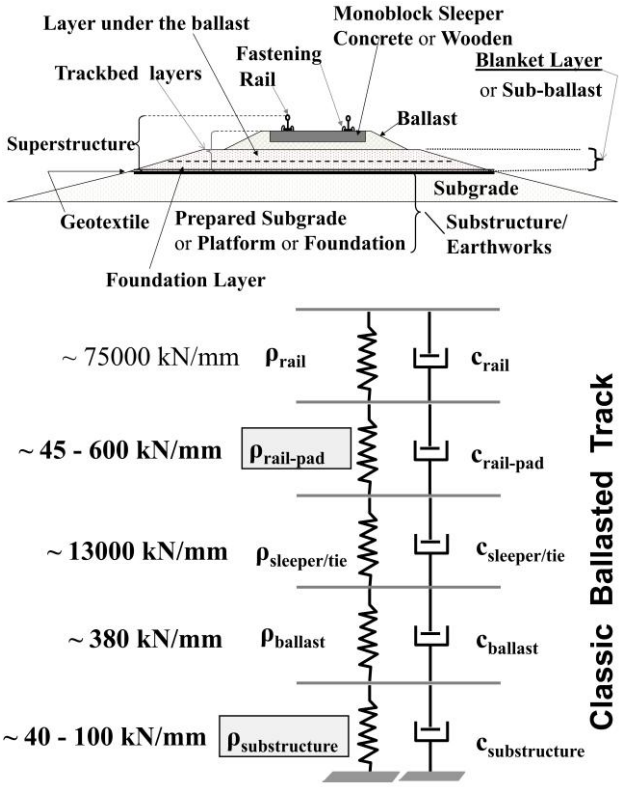

Figure 4. (Upper) Railway Track Cross-section, with the terminology of its layers. (Lower) Cross-section of the Track simulated as an ensemble of springs and dashpots with its characteristic values; the critical spring-constants (of the components/layers) are the fastening-pad's ρ_{pad} and the substructure's $\rho_{substructure}$ [10].

The total Reaction per support point of the Rail, namely per sleeper, is given by the Giannakos Method [[16], [17]]:

$$R_{max} = \frac{1}{2\sqrt[8]{2}} \cdot \sqrt[16]{\left(\frac{\rho_{total} \cdot \ell^3}{E \cdot J}\right)^3} \cdot (Q_{wheel} + Q_\alpha) + \quad (3.3)$$

$$+ (3 \cdot \sqrt{\underbrace{\left(k_\alpha \cdot V \cdot \sqrt[8]{2^6 \cdot (m_{NSM-vehicle} + m_{TRACK})^4 \cdot E \cdot J \cdot \left(\frac{\rho_{total}}{\ell}\right)^3}\right)^2}_{\sigma(\Delta Q_{NSM})}} + \underbrace{\left(\frac{V-40}{1000} \cdot N_L \cdot Q_{wheel}\right)^2}_{\sigma(\Delta Q_{SM})})$$

and the total deflection (static and dynamic) y_{total} (which is equal to $y_{static} + y_{dynamic}$) is given by Eqn (3.4) [[17], 307]]:

$$y_{total} = \bar{A}_{subsidence-dynam} \cdot \left(Q_{wheel-static} + Q_a\right) + \frac{\mu \cdot \left(\sqrt{\sigma^2\left(\Delta Q_{NSM}\right) + \sigma^2\left(\Delta Q_{SM}\right)}\right)}{h_{TRACK}} \quad (3.4)$$

where:

$$h_{TRACK} = \rho_{total-dynamic} = 2\sqrt{2} \cdot \sqrt[4]{E \cdot J \cdot \frac{\rho_{total-static}}{\ell}} \quad (3.5)$$

where E, J the Modulus of Elasticity [in kN/mm] and the Moment of Inertia [in mm^4] of the Rail, and ℓ the distance among the sleepers [in mm], and:

$$A_{subsidence-dynamic} = \frac{1}{2\sqrt{2}} \cdot \sqrt[4]{\frac{\ell^3}{E \cdot J \cdot h_{TRACK}^3}} \quad (3.6)$$

The Giannakos gave results after theoretical calculations -for the ballasted track- verifying and justifying the extended cracking of sleepers observed in a ballasted track; that is the calculation of the Actions/Reactions at each support point of the track with this method is accurate for a probability of occurrence of 99.7%, as it has been repeatedly published on 2002 and in scientific Journals since 2010.

It should be checked for the case of the ballast-less (Slab) Track. Since 1979, professor Eisenmann [et al., [5]] had published measurements for the deflections of a railway track laid with the Rheda-Sengeberg type. The parametric analysis performed with Giannakos method, gave also results in agreement with the measurements (of 1979) on Rheda-Sengeberg slab track in Germany. In this case, for a probability of occurrence of 80% (coefficient μ= 1.43), the Giannakos method gives results that are the same as the measured values in-situ on the Track [17]. In general, the deflections reduce with the increase in the substructure stiffness. The elasticity in the Slab Track structure is mainly provided by the elastic pad of the fastening.

c.- The defects of the Rails due to the production process in the factory create defects of wavelength of 1,60 m on the rail. These defects are owed to the diameter of the rollers (drums) of the rail-production chain in the factory: in the production units of a steel-mill, the forming the rail process occur with the pushing of the mass of hot steel through two rotating rollers in opposite directions. These rollers have a radius of 1,60/(2π) ≈ 0,25 m, or 0,50 m diameter. It should be noted that a Rail Running Surface forming a "*quite perfect line in space*" does not exist in practice, consequently, the rails are produced with a wavelength of approximately 1,60 m.

d.-The defects of random wavelength of the Rail Running Table due to the circulation of the trains,

e.-The defects of random wavelength due to permanent subsidence(s) along the Track.

4 Spectral Density in Random Processes [22]

The paragraphs 4, 5, 6, 7 in this article are derived from [22]; they are cited here to facilitate the understanding of the term "Spectral Density" of random defects on a Railway Track.

The spectral density function S_x is of great importance to the analysis of stochastic processes. Figure 5 illustrates characteristic cases of spectral density of random functions.

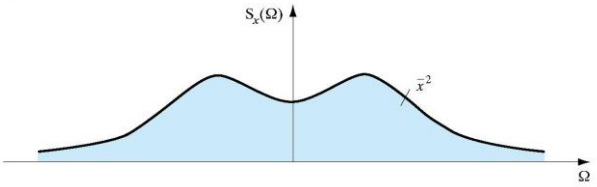

Figure 5. Spectral Density or Power Spectrum $S_x(\Omega)$ and mean square value (average value $\overline{x^2}$) [10].

In the theory of stochastic systems, the spectra are linked to Fourier transforms. For deterministic systems the spectra and the Fourier transformation are used to represent a function as superposition of exponential functions. For random systems (or signals) the concept of spectrum has two interpretations.

a.-The first one includes transforms of averages, and is essentially deterministic.

b.-*The second one includes the representation of the (random) process as a superposition of exponential functions (namely of a sum of infinite sine and cosine functions) with random coefficients*.

The *power spectrum* or *spectral density* of a stochastic system that is described by a function *x(t)* is the Fourier transform of the system's auto-correlation $\Phi_x(t)$.

If *x(t)* represents the excitation and since a stochastic process, at least theoretically, can last indefinitely, it is not a prerequisite that the following equation will apply: $\int_{-\infty}^{+\infty} \left|x(t)\right| \cdot dt < +\infty$ **(4.1)**

even if the mean value $\overline{x} = 0$.

There is greater possibility that $\Phi_x(\Delta t)$ will be finite, that is the absolute value of $\Phi_x(\Delta t)$, which is the area below the curve (Figure 6). From the

continuity of curve $x(t)$, and for small Δt, it can be concluded that both $x(t)$ and $x(t+\Delta t)$ have the same sign and therefore $\Phi_x(\Delta t)$ must increase with time. There is no predictable behavior or relationship in a random process between $x(t)$ and $x(t+\Delta t)$ for great values of Δt. $\Phi_x(\Delta t) \rightarrow 0$ for great values of Δt, because contradictive values may arise in this case.

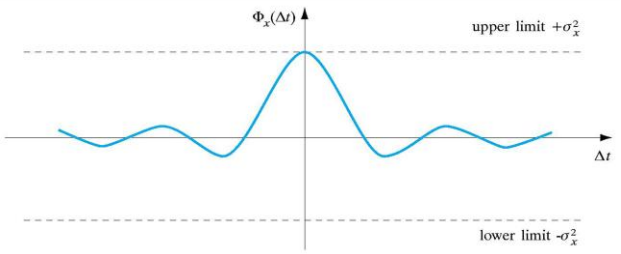

Figure 6. Typical auto-correlation function for stationary process with zero mean value (cf. [[10], 136]).

Let us consider a non-periodic auto-correlation function $\Phi_x(\Delta t)$ that satisfies the equation (4.1). When this equation is valid it allows unlimited use of the Fourier integral (with no restrictions) for the mapping of any function $x(t)$. To calculate this function, we can apply the integral for the calculation of the coefficients of the Fourier series [[10], 121, Eqn. 393],

$$f_i(\omega) = \frac{1}{2\pi} \cdot \int_{-\infty}^{+\infty} P_i(t) \cdot e^{-i \cdot \omega \cdot t} \cdot dt \qquad (4.2)$$

which is the frequency spectrum of the excitation for non-random processes ([[10], 121-122], [[10], 319]) and we get:

$$\Phi_x(\Delta t) = \frac{1}{2\pi} \cdot \int_{-\infty}^{+\infty} S_x(\omega) \cdot e^{i\omega\Delta t} \, d\omega = E\left[x(t+r) \cdot x(t)\right]$$

where:

$$S_x(\omega) = \int_{-\infty}^{+\infty} \Phi_x(\Delta t) \cdot e^{-i\omega\Delta t} \cdot d(\Delta t) \qquad \textbf{(4.3.a-b)}$$

$S_x(\omega)$ is the spectral density function. Furthermore, $S_x(\omega)$ is the Fourier transform of the function $\Phi_x(\Delta t)$ since $\Phi_x(\Delta t)$ is the inverse Fourier transform of $S_x(\omega)$. It should be noted that, if $\Phi_x(\Delta t)$ is defined as $\Phi_x(\Delta t) = E[x(t_1) \cdot x(t_1+\Delta t)]$, then the factor $1/2\pi$ before the integral does not exist in the Eqn. (4.3.a) but in (4.3.b) (see [[9], 269]).

The WIENER-KHINCHIN theorem [[4], 237] is derived from (3.9) and (4.3.a):

$$\sigma^2(x) = \Phi_x(0) = \frac{1}{2\pi} \cdot \int_{-\infty}^{+\infty} S_x(\omega) \cdot d\omega = \bar{x}^2 \qquad (4.4)$$

The shaded area below the spectral density function (Figure 5) *represents the mean square value of the process*.

Using complex numbers in (4.3.b) and the Euler equation for complex numbers, since the imaginary part is eliminated, because $\Phi_x(\Delta t)$ is symmetrical and $\sin(\omega\Delta t)$ is anti-symmetrical with respect to $\Delta t = 0$ and as a result the areas below the anti-symmetrical integral cancel one another [[2], 271], we get:

$$S_x(\omega) = \int_{-\infty}^{+\infty} \Phi_x(\Delta t) \cdot \cos(\omega\Delta t) \cdot d(\Delta t) -$$

$$-i \cdot \int_{-\infty}^{+\infty} \Phi_x(\Delta t) \cdot \sin(\omega\Delta t) \cdot d(\Delta t) =$$

$$= \frac{1}{2\pi} \cdot \int_{-\infty}^{+\infty} \Phi_x(\Delta t) \cdot \cos(\omega\Delta t) \cdot d(\Delta t) \qquad (4.5)$$

It can be easily proved that:

$$S_x(\omega) = S_x(-\omega) \qquad (4.6)$$

The spectral density function is real, it does not contain an imaginary part and is symmetrical around position $\omega = 0$, as the autocorrelation function also is.

5 Strength of an Impulse – Duhamel Integral

We define in general form:

$$I_i = \int_0^{t_1} P_i(t) \cdot dt \qquad (5.1.a)$$

The *Strength (Power) of the excitation Impulse* and the *Strength of a Rectangular excitation Impulse*:

$$I_i = P_0 \cdot t_1 \qquad (5.1.b)$$

Integration of the differential equation without taking into account the damping and under the condition that the phenomenon takes place within a very short time interval (for $k = 1$, $m = 1/\omega_n^2$):

$$\frac{1}{\omega_n^2} u'' + u = P_0, \quad 0 \le t \le t_1, \Rightarrow u'' + \omega_n^2 \cdot u = \omega_n^2 \cdot P_0$$

this leads to the following (for $t = t_1$):

$$\Delta u' = \omega_n^2 \cdot \left(P_0 \cdot t_1 + \int_0^{t_1} u \cdot dt \right) \cong \omega_n^2 \cdot I_i \qquad (5.2)$$

assuming a system initially at rest. Whereas the power of the impulse, even for a short time duration, can attain a significant value owing to a great amplitude of Force P_0, the area below the curve $u(t)$ is practically zero, as a result of the zeroing of the gradient ($t \rightarrow 0$) at the beginning of the curve (for this

reason $\int u \cdot dt \cong 0$).

At the limit $I_i = \lim_{t \to 0} (P_0 \cdot t_1) = k$ (5.3)

where *k* is a finite number.

In this case the applied Force is converted to the *Dirac Impulse*. The Dirac function is defined as P(x) = 0 for $x \neq 0$ and $P(0) = +\infty$ since

$$\int_{-\infty}^{+\infty} P(x) \cdot dx = 1$$

Physicists (and Engineers) are aware that this is not a real function, but rather a symbolic tool. For Electronic Engineers the *Dirac function* is often considered to be the limit of an Impulse, of amplitude Δt and magnitude $1/\Delta t$ when $\Delta t \rightarrow 0$. For more, see ([24]; [29]). Different impulses of short duration with a random form can also be approximately defined by the Eqns (5.1.a and b). Since the strength of impulse I_i is known, the exact fluctuation of *P(t)* is not of interest from a practical point of view.

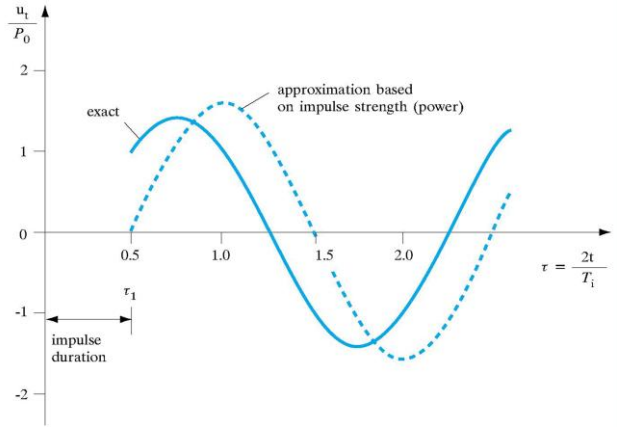

Figure 7. Response to a long duration excitation (cf. [[10], 145]).

An important characteristic of the above theoretical analysis is that the excitation is obtained from Eqn. (5.2). We know that, in every case, the maximum displacement occurs at the phase of free oscillation. By applying the initial conditions:

$u(t_1) = 0$ and $u'(t_1) = \Delta u' = \omega_n^2 \cdot I_i$ (5.4)

The response of the system can be expressed by:

$u(t) = \omega_n \cdot I_i \cdot \sin \omega_n (t - t_1)$ for $t > t_1$ (5.5)

For a *Dirac Impulse* ($t_1 \rightarrow 0$) it is further simplified:

$u(t) = \omega_n \cdot I_i \cdot \sin \omega_n t$ for $t > 0$ (5.6)

Eqn. (5.6) is analytically precise, whereas Eqn. (5.5) is merely an approximation for impulses that are of finite, but short time-duration t_1. We can consider $t_1 < T_i / 4$ as a limit.

$$I_i = P_0 \cdot t_1 = \frac{1}{4} \cdot P_0 \cdot T_i = \frac{\pi}{2} \cdot \frac{P_0}{\omega_n} \quad (5.7)$$

Using Eqn. (5.7) the Eqn. (5.5) gives:

$$u(t) = \frac{\pi}{2} \cdot P_0 \cdot \sin \omega_n (t - t_1) \quad \text{when} \quad t > t_1 \quad (5.8)$$

In Figure 7, we notice, by comparing the precise and the approximate solution –based on the power of the excitation impulse–, a significant deviation for the phase shift, whereas *the maximum amplitude which is of major importance for application to structures*, does not seem to be affected significantly (its deviation does not exceed 11%); see also [[2], 238].

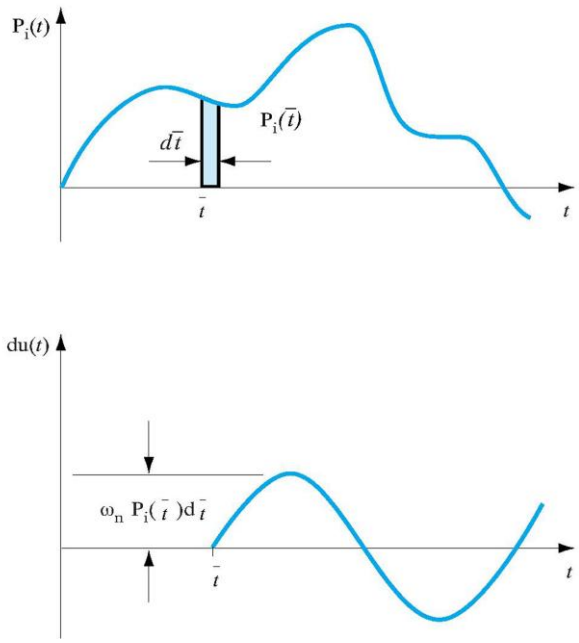

Figure 8. Excitation of generic form, namely, an impulse of finite time-duration (upper illustration) and response (lower illustration); cf. [[10], 146].

Figure 8 illustrates a generic form excitation that can be approached by an infinite sequence of impulses. At time instant $\bar{t}$, an instant infinitesimal impulse is recorded:

$$dI_i = P_i(\bar{t}) \cdot dt \quad (5.9)$$

that causes the response **(5.10)**:

$$du(t) = \omega_n \cdot dI_i \cdot \sin \omega_n (t - \bar{t}) =$$

$$= \omega_n \cdot P_i(\bar{t}) \cdot \sin \omega_n (t - \bar{t}) \cdot dt \quad \text{where} \quad t > \bar{t}$$

Starting from an *at-rest condition*, by integration of the sequence of all impulses, we get the complete response of the system:

$$u(t) = \omega_n \cdot \int_{\bar{t}=0}^{\bar{t}=t} P_i(\bar{t}) \cdot \sin \omega_n (t - \bar{t}) \cdot d\bar{t} \quad (5.10.\mathbf{a}),$$

which is known as ***the Duhamel integral***, and if we pose:

$$h(t - \bar{t}) = \omega_n \cdot \sin \omega_n (t - \bar{t}) \quad (5.10.b),$$

it is transformed to:

$$u(t)=\int_{\bar{t}=0}^{\bar{t}=t} P_i(\bar{t})\cdot h(t-\bar{t})\cdot d\bar{t} \qquad (5.10.c)$$

If the structure does not start from an at-rest condition at $t = 0$, it is necessary to superimpose an additional free oscillation:

$$u(t)=\omega_n\cdot\int_{\bar{t}=0}^{\bar{t}=t} P_i(\bar{t})\cdot\sin\omega_n(t-\bar{t})\cdot d\bar{t}+\frac{u'(0)}{\omega_n}\cdot\sin\omega_n t+$$
$$+u(0)\cdot\cos\omega_n t \qquad (5.11\ 36)$$

Numerical calculation methods, such as the Romberg, Gauss, Simpson, etc, have been developed for the calculation of Duhamel integral.

In any case we can assume that the phenomenon starts at $t = 0$.

6 Random excitation in a system with damping, with one degree of freedom

From the *Duhamel integral* Eqns (5.10) we find the response in the time domain. The basic second order differential equation of motion which is applied to the system "Railway Vehicle-Railway Track" (see [11], [12]) is:

$$u''+2\zeta_i\cdot\omega_n\cdot u'+\omega_n^2\cdot u=\omega_n^2\cdot P_i(t) \qquad (6.1)$$

Where $P_i(t)$ is presumed to be an ergodic random force with a mean value equal to zero. The mathematical expression of the term $P_i(t)$ is [[10], 147]:

$$P_i(t)=\frac{P_0}{k}\cdot e^{i\omega t} \qquad (6.2)$$

Using the *Duhamel integral* we can calculate the response of the system, which represents the response of the system to a *unitary Dirac Impulse* [see [21]]. We should calculate this response.

(a).- $P_i(t) = 0$ and we derive:

$$u(t)_i=e^{-\omega_n\cdot\zeta_i\cdot t}\cdot(a_i\cdot\sin(\omega_{D_i}\cdot t)+b_i\cdot\cos(\omega_{D_i}\cdot t)) \quad (6.3.1),$$

where: $\omega_{D_i}=\omega_n\cdot\sqrt{1-\zeta_i^2}$ (6.3.4),

if $\zeta_i < 1$ (*under-critical* damping).

$$u(t)_i=e^{-\omega_n t}(a_i+b_i\cdot t) \qquad (6.3.2),$$

if $\zeta_i = 1$ (*critical* damping).

$$u(t)_i=a_i\cdot e^{-\omega_n\cdot(\zeta_i-\sqrt{\zeta_i^2-1})\cdot t}+b_i\cdot e^{-\omega_n\cdot(\zeta_i+\sqrt{\zeta_i^2-1})\cdot t} \quad (6.3.3),$$

if $\zeta_i > 1$ (*over-critical* damping):

Proportionally to the above, which applies for a free system without damping, we can examine the equation and find a solution for an under-critically damped system, for which the initial conditions are u(0) and u′(0) (see [[10], 100, Eqn. 3.3.5]):

The particular solution becomes (**6.4.1**):

$$b_i=u(0),\ a_i=\frac{u'(0)+\omega_n\zeta_i u(0)}{\omega_n\sqrt{1-\zeta_i^2}}=\frac{u'(0)+\omega_n\zeta_i u(0)}{\omega_{D_i}}$$

and (**6.4.2**),

$$u(t)=e^{-\omega_n\zeta_i\cdot t}\cdot\left(\frac{u'(0)+\omega_n\zeta_i\cdot u(0)}{\omega_n\sqrt{1-\zeta_i^2}}\cdot\sin\omega_n\sqrt{1-\zeta_i^2}\cdot t+\right.$$
$$\left.+u(0)\cdot\cos\omega_n\sqrt{1-\zeta_i^2}\cdot t\right)=$$
$$=e^{-\omega_n\zeta_i t}\cdot\left(\frac{u'(0)+\omega_n\zeta_i u(0)}{\omega_{D_i}}\cdot\sin\omega_{D_i}t+u(0)\cdot\cos\omega_{D_i}t\right)$$

(b).- If we consider a forced oscillation $P_i(t) \neq 0$ with damping, the solution of the differential equation (6.1) now consists of two parts: a homogenous part which we have come across in Eqns. (6.3.1) to (6.3.3) in this paragraph, and a particular solution up that depends on the type of excitation (**6.4.3a**):

$$u(t)_i=e^{-\omega_n\cdot\zeta_i\cdot t}\cdot(a_i\cdot\sin(\omega_{D_i}\cdot t)+b_i\cdot\cos(\omega_{D_i}\cdot t))+u_p(t)_i$$

this equation applies to the most common types of under-critical damping.

If we pose in Eqn. (6.2) $P_0/k = 1$, then:

$$P_i=e^{i\omega t}=\cos\omega t+i\cdot\sin\omega t \qquad (6.4.3b)$$

and its response:

$$u(t)=F_i\cdot e^{i\omega t} \qquad (6.4.3c)$$

where:

$$F_i=\frac{1}{1-\left(\frac{\omega}{\omega_n}\right)^2+i\cdot 2\zeta_i\cdot\left(\frac{\omega}{\omega_n}\right)} \qquad (6.4.3d)$$

Recalling from the theory of complex functions:

$$\frac{1}{a+ib}=\frac{1}{r(\cos\varphi+i\sin\varphi)}=\frac{1}{r}\cdot e^{-i\varphi} \qquad (6.4.4)$$

where:

$$r=\left(a^2+b^2\right)^{1/2},\quad \varphi=\tan^{-1}\frac{b}{a} \qquad (6.4.5)$$

Value $1/r$ gives the absolute value of the complex frequency response characteristic F_i and the response factor of displacement (amplification factor) R_{d_i}:

$$R_{d_i}=\left(\left[1-\left(\frac{\omega}{\omega_n}\right)^2\right]^2+\left[2\zeta_i\cdot\left(\frac{\omega}{\omega_n}\right)\right]^2\right)^{-1/2} \qquad (6.4.6)$$

Angle φ_i specifies the phase shift:

$$\varphi_i=\tan^{-1}\frac{2\zeta_i\cdot\frac{\omega}{\omega_n}}{1-\left(\frac{\omega}{\omega_n}\right)^2} \qquad (6.4.7)$$

The particular solution for an excitation of the form (6.4.3b) is:

$$u_p(t) = R_{d_i} \cdot e^{-i\varphi_i} \cdot e^{i\cdot\omega t} = R_{d_i} \cdot e^{i(\omega t-\varphi_i)} =$$

$$= R_{d_i} \cdot \left(\cos(\omega t-\varphi_i) + i\cdot\sin(\omega t-\varphi_i)\right) \quad (6.4.8)$$

As it is well known, the homogenous solution of the system with damping, is gradually damped and the particular solution (6.4.8) represents the oscillation of the steady state condition of the system. The damping determines the phase shift of the system's response through Eqn. (6.4.7), which -for a system without damping- is 0 or π. Amplification factor R_{d_i} *always remains finite, even in the case of resonance (ω = ωn).*

After the above analysis, we come back to the solution of Eqn. (6.1) and (5.10.b) that represents the response to a *Dirac impulse*. From the particular solution (**6.4.2**), setting as initial conditions:

$$u(0) = 0, \quad \dot{u}(0) = \omega_n^2 \cdot \int P_i(t)\cdot dt = \omega_n^2 \cdot 1 \quad (6.4.9)$$

that corresponds to the *Dirac impulse*, introducing the necessary phase shift and assuming a weak damping, we have the solution (the only difference to the response is that it decreases exponentially):

$$h(t-\bar{t}) = \frac{\omega_n}{\sqrt{1-\zeta^2}} \cdot e^{-\omega_n\zeta(t-\bar{t})} \cdot \sin\left(\omega_{D_i}(t-\bar{t})\right) \quad (6.4.10)$$

this formula can be applied up to the critical damping $\zeta_i = 1$. For $\zeta_i = 0$ the solution (6.4.10) turns into (5.35.b). Both Eqns. (6.4.10) and (5.10.b) must be complemented by:

$$h(t-\bar{t}) = 0 \quad \text{for} \quad t < \bar{t} \quad (6.4.11)$$

since no response can exist before the application of *the (unitary) Dirac impulse*.

Nevertheless, it should be noted that random excitation Pi (t) does not start at instant $\bar{t}$, but it could go on –at least in theory– even before $\bar{t}$, for an indefinite period of time. Eqn. (5.10.b) can be written (*Duhamel integral*):

$$u(t) = \int_{\bar{t}=-\infty}^{\bar{t}=t} P_i(\bar{t})\cdot h(t-\bar{t})\cdot d\bar{t} = \quad (6.4.12)$$

$$= \int_{\bar{t}=-\infty}^{\bar{t}=+\infty} P_i(\bar{t})\cdot h(t-\bar{t})\cdot d\bar{t} = \int_{-\infty}^{+\infty} h(\theta)\cdot P_i(t-\theta)\cdot d\theta$$

where $\theta = t - \bar{t}$.

The mean value of the response is:

$$\bar{u} = E[u] = E\left[\int_{-\infty}^{+\infty} h(\theta)\cdot P_i(t-\theta)\cdot d\theta\right] =$$

$$= \int_{-\infty}^{+\infty} h(\theta)\cdot E\left[P_i(t-\theta)\right]\cdot d\theta =$$

$$= \int_{-\infty}^{+\infty} h(\theta)\cdot \bar{P}_i \cdot d\theta = \bar{P}_i \int_{-\infty}^{+\infty} h(\theta)\cdot d\theta \quad (6.4.13)$$

Here it should be noted that the calculation of the mean value for an ergodic process *u(t)* is done on the axis of time *t.* But, in this case, since only $P_i(t - \theta)$ depends on time *t,* the mean value can be extracted before the integration. Since excitation function $P_i(t)$ is also ergodic and stationary, *its mean value* $\bar{P}_i$ has to be independent of time. Hence the mean value in (6.4.13) is obtained. A very important rule is derived from the above: if the mean value of the excitation is zero, then the mean value of the response is also zero.

The next step is the calculation of the response autocorrelation function. Here we also face an expectation value:

$$\Phi_u(\Delta t) = E\left[u(t)\cdot u(t+\Delta t)\right] = \quad (6.4.14)$$

$$= E\left[\left(\int_{-\infty}^{+\infty} h(\theta_1)\cdot P(t-\theta_1)\cdot d\theta_1\right)\cdot\left(\int_{-\infty}^{+\infty} h(\theta_2)\cdot P_i(t+\Delta t-\theta_2)\cdot d\theta_2\right)\right] =$$

$$= E\left[\int_{-\infty}^{+\infty}\int_{-\infty}^{+\infty} h(\theta_1)\cdot h(\theta_2)\cdot P_i(t-\theta_1)\cdot P_i(t-\theta_2+\Delta t)d\theta_1\cdot d\theta_2\right] =$$

$$= \int_{-\infty}^{+\infty}\int_{-\infty}^{+\infty} h(\theta_1)\cdot h(\theta_2)\, E\left[P_i(t-\theta_1)P_i(t-\theta_2+\Delta t)\right]d\theta_1 d\theta_2 =$$

$$= \int_{-\infty}^{+\infty}\int_{-\infty}^{+\infty} h(\theta_1)\cdot h(\theta_2)\cdot \Phi_p(\Delta t+\theta_1-\theta_2)\cdot d\theta_1\cdot d\theta_2$$

Here Φ_p is the excitation autocorrelation function and Φ_u is the response autocorrelation function. In practice, their detailed calculation is difficult.

From equations (6.4.13) and (6.4.14) it can be derived that response *u(t)* is also stationary for a stationary excitation $P_i(t)$, since neither the mean value $\bar{u}$ nor autocorrelation function $\Phi_u(\Delta t)$ depend on time *t*.

The transformation of spectral density S_p of the excitation into spectral density S_u of the response can be easily calculated. For this purpose, we use the definition of the Spectral Density (Eqn. 4.3.a-b) and the Eqn. (6.4.14) and we calculate the corresponding Spectral Density from the autocorrelation function:

$$S_u(\omega) = \frac{1}{2\pi}\int_{\Delta t=-\infty}^{+\infty} \Phi_u(\Delta t)\cdot e^{-i\omega\Delta t}\cdot d(\Delta t) = \quad (6.4.15)$$

$$= \frac{1}{2\pi}\int_{\Delta t=-\infty}^{+\infty}\int_{\theta_1=-\infty}^{+\infty}\int_{\theta_2=-\infty}^{+\infty} h(\theta_1)\cdot h(\theta_2)\cdot\Phi_p(\Delta t+\theta_1-\theta_2)\cdot d\theta_2\cdot d\theta_1\cdot e^{-i\omega\Delta t}\cdot d(\Delta t) =$$

$$= \int_{-\infty}^{+\infty}\int_{-\infty}^{+\infty} h(\theta_1)\cdot h(\theta_2)\cdot\left(\frac{1}{2\pi}\int_{\Delta t=-\infty}^{+\infty}\Phi_p(\Delta t+\theta_1-\theta_2)\cdot e^{-i\omega\Delta t}\cdot d(\Delta t)\right)\cdot d\theta_1\cdot d\theta_2 =$$

$$= S_p(\omega)\cdot\int_{-\infty}^{+\infty}\int_{-\infty}^{+\infty} h(\theta_1)\cdot h(\theta_2)\cdot e^{-i\omega(\theta_2-\theta_1)}\cdot d\theta_1\cdot d\theta_2$$

The statistical measurements taken for the response also contain some expressions with integrals. Nevertheless, they can be simplified through the Fourier integral (transform) method,

producing impressive results (for an easy calculation of the Fourier integral, see [[27], paragr. 4-1]). Eqn. (6.4.12) is the Duhamel integral and the response in the time domain. If we apply the Fourier transformation as in the non-periodic functions of Eqns. (4.2) to (4.3.a-b) to an excitation impulse with unit value at $\theta = 0$, then we derive the following response:

$$h(\theta) = \int_{-\infty}^{+\infty} F_i(\omega) \cdot f_i(\omega) \cdot e^{i\omega\theta} \cdot d\omega \qquad (6.4.16)$$

which is the response in the *frequency domain*, where the *complex characteristic response frequency*:

$$F_i(\omega) = \frac{1}{1 - \left(\frac{\omega}{\omega_n}\right)^2 + i \cdot 2\zeta_i \cdot \frac{\omega}{\omega_n}} \qquad (6.4.17)$$

and the frequency spectrum of the excitation impulse becomes (introducing a new time variable $\theta = t - \bar{t}$) [see [[10], 153, n. 21, 119] and [[3], 98-9]):

$$f_i(\omega) = \frac{1}{2\pi} \cdot \int_{-\infty}^{+\infty} P_i \cdot e^{-i\omega\theta} \cdot d\theta = \frac{1}{2\pi} \qquad (6.4.18)$$

We get the above result because Pi fluctuates only inside a range of small values of θ, where $e^{-i\omega\theta} \cong 1$. Then the integral gives the impulse and then it is indeed 1. From Eqn. (6.4.16) we find:

$$h(\theta) = \frac{1}{2\pi} \cdot \int_{-\infty}^{+\infty} F_i(\omega) \cdot e^{-i\omega\theta} \cdot d\theta \qquad (6.4.19)$$

The comparison with equations (4.2) to (4.4) gives the expression $F_i(\omega)/2\pi$ for the Fourier transform of function $h(\theta)$. According to Eqn . (4.4) we have:

$$F_i(\omega) = \int_{-\infty}^{+\infty} h(\theta) \cdot e^{-i\omega\theta} \cdot d\theta \qquad (6.4.20)$$

where the complex characteristic frequency is defined by the simple Eqn (6.4.17). Hence the integrals with infinite limits can be elegantly calculated and, instead of Eqn. (6.4.13) we get for the mean value of the response, when $\omega = 0$:

$$\bar{u} = \overline{P_i} \cdot F(0) = \overline{P_i} \qquad (6.4.21)$$

For the Eqn. (6.4.15) we have:

$$\int_{-\infty}^{+\infty}\int_{-\infty}^{+\infty} h(\theta_1) \cdot h(\theta_2) \cdot e^{-i\omega(\theta_2 - \theta_1)} \cdot d\theta_1 \cdot d\theta_2 =$$

$$= \int_{-\infty}^{+\infty} h(\theta) \cdot e^{+i\omega\theta} \cdot d\theta \cdot \int_{-\infty}^{+\infty} h(\theta) \cdot e^{-i\omega\theta} \cdot d\theta =$$

$$= F_i^*(\omega) \cdot F_i(\omega) = R_d^2 \qquad (6.4.22)$$

here F_i^* is the complex conjugate of F_i and R_d is the real amplification factor of equation (6.4.15), that coincides with the modulus of the complex characteristic frequency.

We have:

$$R_d^2 = \left(\left[1 - \left(\frac{\omega}{\omega_n} \right)^2 \right]^2 + \left[2\zeta_i \cdot \frac{\omega}{\omega_n} \right]^2 \right)^{-1} \qquad (6.4.23)$$

Equation (6.4.15) can be now written into the simplified form:

$$S_u(\omega) = R_d^2 \cdot S_p(\omega) \qquad (6.4.24)$$

7 Transformation Functions in Time and Frequency domains

From the *Duhamel integral* (5.35.a, 5.35.c, 6.4.12) we find the response:

$$u(t) = \int_{+\infty}^{t} P(t) \cdot h(t - \tau) \cdot dt \qquad (7.1)$$

that applies for the time domain, whereas for the frequency domain:

$$u(t) = \int_{-\infty}^{+\infty} F_i(\omega) \cdot f_i(\omega) \cdot e^{-i\omega \cdot t} \cdot d\omega \qquad (7.2)$$

which derives from Eqn. (6.4.16); we should underline that we use the general form $P_i(t)$ instead of a unitary load (as the *Dirac Impulse*). From Eqn. (6.4.18) we derive:

$$f_i(\omega) = \frac{1}{2\pi} \int_{-\infty}^{+\infty} P_i(t) e^{-i\omega \cdot t} dt \qquad (7.3)$$

and bearing in mind that θ is a time variable, from Eqn. (6.4.17) we have the frequency response function, which is a complex function:

$$F_i(\omega) = \frac{1}{1 - \left(\frac{\omega}{\omega_n}\right)^2 + i \cdot 2\zeta_i \cdot \frac{\omega}{\omega_n}} \qquad (7.4)$$

and also the response function to a unitary impulse (from Eqn. 6.4.10):

$$h(t - \bar{t}) = \frac{\omega_n}{\sqrt{1 - \zeta^2}} \cdot e^{-\omega_n \zeta (t - \bar{t})} \cdot \sin\left(\omega_{D_i} (t - \bar{t})\right) \qquad (7.5)$$

It is characteristic that $F_i(\omega)$ and $h(t - \bar{t})$ are related through the *Fourier transform* and the *inverse Fourier transform*. From Eqn. (6.4.20) we have (**7.6**):

$$F_i(\omega) = \int_{-\infty}^{+\infty} h(\theta) \cdot e^{-i\omega\theta} \cdot d\theta = \int_{-\infty}^{+\infty} h(t - \bar{t}) \cdot e^{-i\omega(t - \bar{t})} \cdot dt = H(\nu)$$

and from Eqn. (6.4.19), we have (**7.7**):

$$h(\theta) = \frac{1}{2\pi} \cdot \int_{-\infty}^{+\infty} F_i(\omega) \cdot e^{-i\omega\theta} \cdot d\theta = \frac{1}{2\pi} \int_{-\infty}^{+\infty} F_i(\omega) \cdot e^{-i\omega(t - \bar{t})} \cdot dt$$

8 Relationship between Excitation-Response Spectral Densities: Track Defects and Motion of the Vehicle

If we have the system "Railway Vehicle-Railway Track" then the condition and the position in space of the rail running table is the excitation (Input) and the movement of the vehicle is the response (Output).

From Eqn. (6.4.15) we have (**8.1**):

$$S_u(\omega) = S_p(\omega) \int_{-\infty}^{+\infty} h(\theta_1) \cdot e^{-i\omega\cdot\theta_1} \cdot `d\theta_1 \cdot \int_{-\infty}^{+\infty} h(\theta_2) \cdot e^{i\omega\cdot\theta_2} \cdot d\theta_2$$

and using Eqns. (7.6) and (8.1), we find Eqn. (**8.2**) below (see also [[5], Ch.2]):

$$S_u(\omega) = H(-i\omega) \cdot H(i\omega) \cdot S_p(\omega) = |H(i\omega)|^2 \cdot S_p(\omega)$$

where frequency ν has two parts one real and one imaginary.

However, *the spectral density function is real, it does not contain an imaginary part* (see paragraph 4); the Spectral Density of the response (output) Su is related to the Spectral Density of the excitation (input) with a real number $|H(i\omega)|^2$.

Consequently, if we find or measure the Spectral Density of the input we can calculate the Spectral density of the output.

In the case of the Track defects, it should be clarified that different wavelengths address different vehicles' responses depending on the length of the cord/base of measurement. This is of decisive importance for the wavelengths of 30 – 33 m, which are characteristic for very High Speed Lines ([19], [20]). In the real tracks, the forms of the defects are random with wavelengths from few centimetres to 100 m. The defects constitute the "Input" in the system "Vehicle-Track" since the deflection y and the Action/Reaction R of each support point of the rail/sleeper are the "Output" or "Response" of the system. The accuracy of the measurements of the defects is of utmost importance for the calculation of the deflection y and the Reaction R; this accuracy, due to the bases of the measuring devices/vehicles, is fluctuating. Thus we should pass from the space-time domain to the frequencies' domain through the Fourier transform, in order to use the power spectral density of the defects, especially for defects, with (long) wavelength, larger than the measuring base of the vehicle.

In the case of random defects then we do not use the function f(x) but its Fourier transform:

$$F(\Omega) = \int_{-\infty}^{+\infty} f(x) \cdot e^{-i\Omega x} \cdot dx \qquad (8.3)$$

In practice we don't know the function of real defects y(x) but the measured values f(x), from the recording vehicle, and we imply that:

$$S_Z(\Omega) = S_{INPUT}(\Omega) = \frac{S_F(\Omega)}{|K(\Omega)|^2} = \frac{S_{OUTPUT}(\Omega)}{|K(\Omega)|^2} \qquad (8.4)$$

where $S_Z(\Omega)$ is the spectral density of the Fourier transform of the real defects (input in the track recording vehicle), $S_F(\Omega)$ is the spectral density of the Fourier transform of the measured values (output) and $K(\Omega)$ is a complex transfer function (of the Recording Vehicle/Car), called frequency response function, transforming the measured values of defects to the real values. For very High-Speed Lines we should analyze the system "railway track – railway vehicle". The calculation of the spectrum of track defects is described in [[28] (paragr. 6) and [6] (155-158); for the Quality of Track see [7]].

9 Dynamic Vertical Stresses on the Trackbed - Excitation Spectra of the System

In this paragraph we analyze real graphs of Spectral Densities of (different wavelengths) Track Defects in relation to the imposed excitation frequencies and the actions on Track as response to the excitation.

When dynamic phenomena are examined -in addition to its function as the support of the vehicle, as it was depicted by the precedent static analysis- the Track operates as a suspension too, the counterpart of the vehicle's suspension in the vertical axis (*z-z*).

It is understood that, in both cases, the developed stresses will depend, on the one hand, on the mechanical characteristics (stiffness, damping) of the systems -track and vehicle-, and on the excitation which results from the movement of the vehicle on the Track.

While a significant random part of the total Load can be attributed to the mechanical characteristics at a given point (x_0), particularly for the Track, despite the large number of studies and measurements already carried out, our knowledge now is much better on the excitation undergone by the system, thanks to the evolution of these measurement techniques.

The Recording Vehicles of the condition of the Track, used by the SNCF for over thirty years, have indeed been equipped with a recording system that provides access to the powerful analytical tool of computer signal processing. Other measuring vehicles have also made it possible to broaden the band of frequencies in which the excitation -due to the geometric condition of the Track- can now be measured; this band extends from defects of a few centimeters wavelength up to approximately fifty or more meters (wavelength).

The visual analysis of the recording graphs of the Track geometry, which remains the basis of Track-maintenance, was therefore complemented by frequency analysis in the form of the calculation of

power Spectral density of geometric defects of the Track.

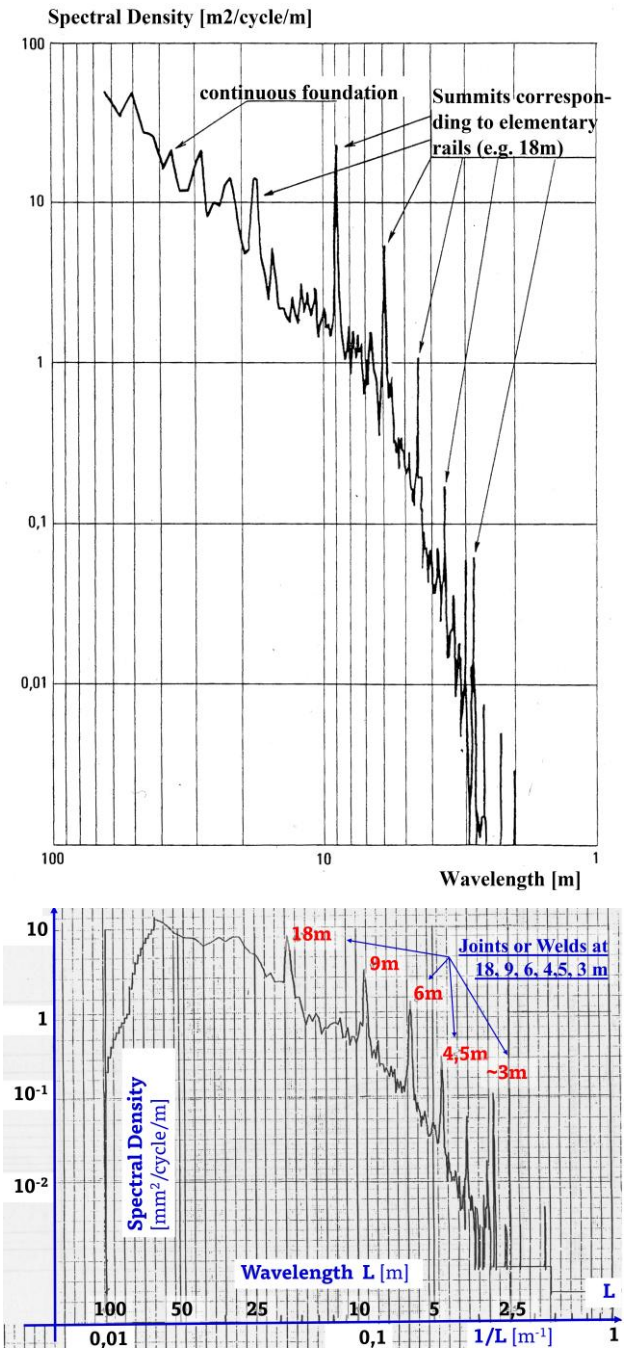

Figure 9. (Upper) Graph of a typical Spectral Density [m^2/cycle/m] calculated from a Recording of a Track Section. The summits/peaks are situated for different wavelengths. (Lower) An example of a graph of Spectral Density [mm^2/cycle/m] calculated from a Recording of a specific Track Section with summits/peaks precisely at the wavelengths of 18m, 9m, 6m and 4,5m, which are the typical lengths of pieces-of-rails used in a Track [see: [9], [8], [1]].

In the analysis and evaluation of a recording of a given length of a Track-section and of each-one of the characteristic parameters of the Track geometry (leveling, alignment, cant, etc.), we can -by calculating the square of the absolute value of the Fourier Transform of this signal (which must have finite energy)- obtain a representation of the Spectral density of the considered defect of each of the above parameters, characteristic of the energy density contained in the signal at a given frequency. If the defect is, for example, expressed in mm of variation of the rail position relative to an absolute or relative basis, the spectrum:

a_1.-A continuous spectrum (Fig. 9-Upper), decreasing towards shorter wavelengths (a "pink" noise, as electricians would say), is characteristic of random track defects. This spectrum has been explored in practice between 100 m and 3 cm. Current studies, primarily aimed at determining whether this pattern corresponds to a physical reality, seem to indicate that we are dealing with two different phenomena, with the "cut-off" wavelength occurring around 6 m.

a_2.- A spectrum with almost equidistant "summits/peaks" characteristic of the length of the elementary bars. This spectrum is obviously predominant for Tracks with joints (or welds that are not perfectly welded) and is very attenuated for CWRs (Continuously Welded Rails -Track without joints). It can also originate from the track bed's history, which in some cases may "record/remember" the position of old periodic faults, such as joints, or from the repetition of localized Track leveling which has altered the Trackbed's characteristics. We see (Fig. 9-Lower) that there are summits/peaks at 18m (the length of the elementary pieces of rail as they are produced in the factory) and also 9m, 6m, 4,5m and ~3m, which are the lengths of rail-pieces used in the maintenance works on Track (repairing the broken welds, final welds after the Liberation of Stresses etc., in Continuously Welded Rails [CWR]).

b.- A second group of spectra, characteristic of rail manufacturing procedure and, generally, a consequence of the final alignment process of rails in the production-chain of rails in the factory. This is located over short wavelengths: 1,60 to 1,80 m in France, but it can reach up to 3 m for other countries' factories. On a 1,60 m measurement-base (chord), we measure essentially the manufacturing defects of the rail (Fig. 10) which are attributed to their straightening in the roller machine, at the end of production-chain in the factory, which produces the rails; this defect typically appears in the form of a quasi-sinusoidal curve with a wavelength varying -normally- between 1,7 and 1,8 m (in France)

depending on the diameter of the straightening rollers [[1], [30] [9]].

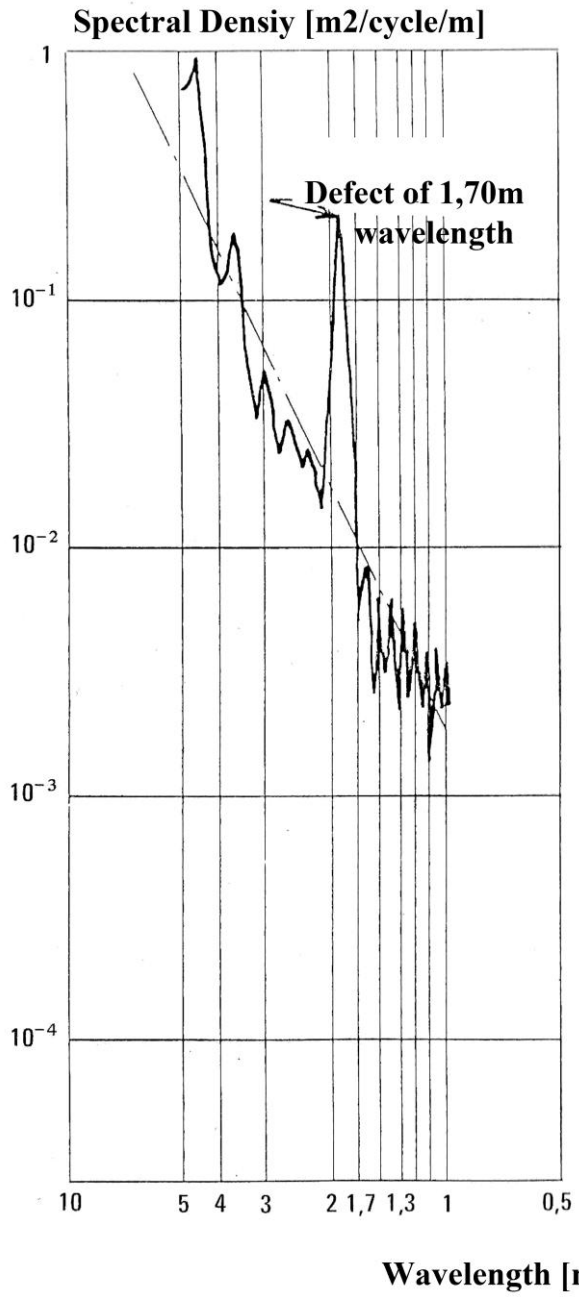

Figure 10. Graph of a typical Spectral Density [m^2/cycle/m] calculated from a Recording of a Track Section. The summit/peak is situated for a wavelength of 1,70 m; this represents a defect owed to the production of the rail in the factory [see: [[9], [8]], [1]].

In Figs. 9, 10, 11 the graphs of the Spectral Densities are presented, as they were contributed by the experts of the SNCF during the meetings (Cooperation OSE/SNCF, see [[25], [26]]) on 1988-1989; they are included in [9] (Meetings' Minutes) and [8] (Report of the Experts' Committee of OSE); all of them (except Fig. 9-Lower) are presented also in [1].

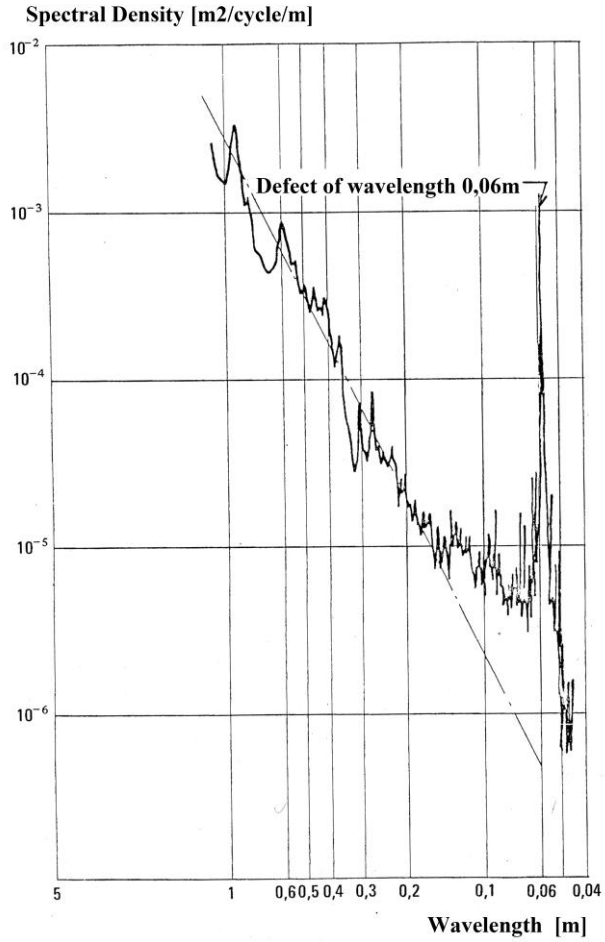

Figure 11. Graph of a typical Spectral Density [m^2/cycle/m] calculated from a Recording of a Track Section. The summit/peak is situated for a wavelength of 0,06 m (undulatory wear) [see: [[9], [8], [1]].

c.-A third group of spectra, characteristic of what is called "undulatory wear" caused by traffic and generally located between 10 and 5 cm (but sometimes at 30 or 70 cm or even 2 cm). On a 400 mm measurement-basis (chord), we measure this defect ("undulatory wear") of short wavelength generated by train traffic but also -as all indications suggest- is related to the phenomena of relative slippage of the wheel on the Rail Running Table; undoubtedly the undulatory wear is excited at certain specific frequencies: at the natural vibration frequencies (eigenfrequencies) of the wheel and the rail. Indeed, we observe a modulation of this undulatory wear defect by the 1,6 m diameter defect when it exists; this fact proves the link between undulatory wear of short wavelength and dynamic wheel loads.

Within the wavelength-range thus covered, extending from 0,02 to 3 m, the defect spectrum consists, as at longer wavelengths too, of a continu-

ous, seemingly random foundation, decreasing as the 3rd power of the spatial frequency, overlaid with characteristic lines of the afore-mentioned defects.

10 The Response of the Track-Vehicle system to the Spectra of Excitations

The response is consisting, at the Track level, of dynamic overloads ($Q_{dynamic}$), that are superimposed on the Reaction (R_{static}) at each support-point (sleeper) of the rails; the R_{static} is derived from the nominal axle-load [Q_{axle}] (or the load of the wheel [$Q_{wheel}=Q_{axle}/2$], if we examine each rail separately for simplicity reasons), after the distribution of the wheel-load among the adjacent sleepers to the support-point (sleeper) under examination.

Moreover, to this $Q_{wheel\text{-}static}$ a quasi-static (or semi-static) load on curves, due to excessive or insufficient cant, which is also distributed to the adjacent sleepers as the Q_{static}.

Cant, on a curve in a Railway Track, is the difference between the (absolute) elevations of the two Rail Running Tables (of the left and the right rail along the Track, see Fig. 12-Lower the difference *h*); cant is essential for maintaining stability and safety for trains on curves. Cant helps counteract the total centrifugal force -or a percentage of it-, allowing trains to move through curves at higher speeds without excessive wheel flange contact with the rails, which minimizes friction and wear. In Fig. 12-Upper, the Track has no superelevation (the two Rail Running Tables have exactly the same absolute elevations.

A vehicle enters a curve guided by the wheel bandages. The theoretical cant mV^2/g fully balances the centrifugal force (see Fig. 12). However, through a Track curve, both fast (passenger) and slow moving (freight) trains are circulating, the cant h given to a curve is less than the theoretical one ($h_{theoretic}$) and there is also a cant deficiency *d* for the passenger trains and an excess δ for the freight trains. In Fig. 12, let the vehicle to move at speed V [in km/h, since v in m/sec], on a curve of radius R and cant h, the unbalanced centrifugal acceleration is:

$$\gamma_{unbalanced} = \frac{v^2}{R} - \frac{g \cdot h}{e}, \qquad h_{theoretic} = \frac{e \cdot v^2}{g \cdot R} = \frac{11{,}8 \cdot V^2}{R}$$

Where: v speed in m/sec, V speed in km/h, R radius in m, g the gravitational acceleration 9,81 m/sec^2, h the superelevation in mm and e the Track gauge.

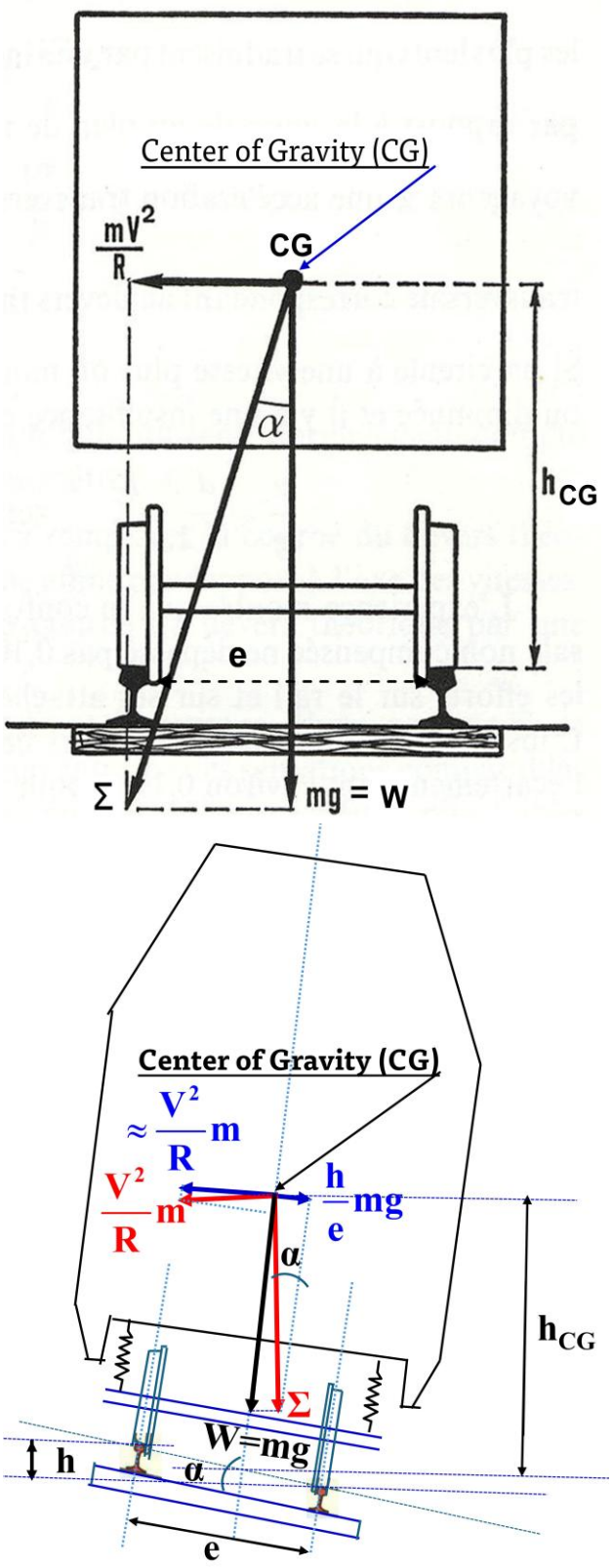

Figure 12. Vehicle on a curve (upper) without superelevation, (Lower) with superelevation.

Cant deficiency *d* is the difference between the theoretic $h_{theoretic}$ and the real superelevation *h*:

$$d = h_{theoretic} - h_{real} = \frac{e \cdot v^2}{g \cdot R} - h_{real} = 11{,}8 \cdot \frac{V_{\max}^2}{R} - h_{real}$$

$$\gamma_{unbalanced} = \frac{g \cdot d}{e}$$

the latter relates the cant deficiency d with $\gamma_{unbalanced}$, in analogy to the $\gamma_{theoretic}$.

In Fig. 12-Upper, the vehicle circulates on a curve of radius R with $h=0$ (zero superelevation). On the vehicle the Weight W acts plus the centrifugal Force equal to mV^2/R and these two Forces are added as vectors and the resultant (CG-Σ) is a quasi-apparent weight. In order for the vehicle not to exert a lateral force, the outer rail of the curve must be raised by a superelevation h given by the relationship:

$$h_{theoretic} = e \cdot \tan \hat{a} = \frac{e \cdot V^2}{g \cdot R}$$

If the lateral acceleration is not balanced completely (either centrifugal for fast trains or centripetal for slow trains) we have either cant deficiency d or excess of superelevation δ, which leeds to inclinations either dg/e or $\delta g/e$.

If γ_1 is the lateral acceleration corresponding to the theoretic superelevation (for completely balanced acceleration) then:

$$\gamma_1 = \frac{V^2}{R} \Rightarrow \frac{\gamma_1}{g} = \frac{V^2}{g \cdot R} = \frac{\frac{d \cdot g}{e}}{g} = \frac{d}{e}$$

and the total γ comprises γ_1 and $\gamma_{\text{unbalanced}}$.

$$\frac{\gamma}{g} = \frac{h+d}{e} \Rightarrow \gamma = \frac{h \cdot g}{e} + \frac{d \cdot g}{e} = \gamma_1 + \gamma_{unbalanced}$$

In Fig. 12-Lower at the limit just before the overturning of the vehicle, its Weight (W) will pass (in the vertical direction) through the lower rail. The angle α -in this case- has:

$$\tan \hat{\alpha} = \frac{\frac{e}{2}}{h_{CG}} = \frac{e}{2 \cdot h_{CG}} \Rightarrow cot\hat{\alpha} = \frac{2 \cdot h_{CG}}{e}$$

Consequently, from Fig. 12-Lower we see that the horizontal Force due to cant deficiency α gives an additional Force, vertical to the inclined -due to the superelevation- level:

$$Q_\alpha = m \cdot \gamma_{unbalanced} \cdot \cot \hat{\alpha} = Q_{wheel} \cdot \frac{\alpha}{e} \cdot \cot \hat{\alpha} =$$

$$= Q_{wheel} \cdot \frac{\alpha}{e} \cdot \frac{2 \cdot h_{CG}}{e} \Rightarrow$$

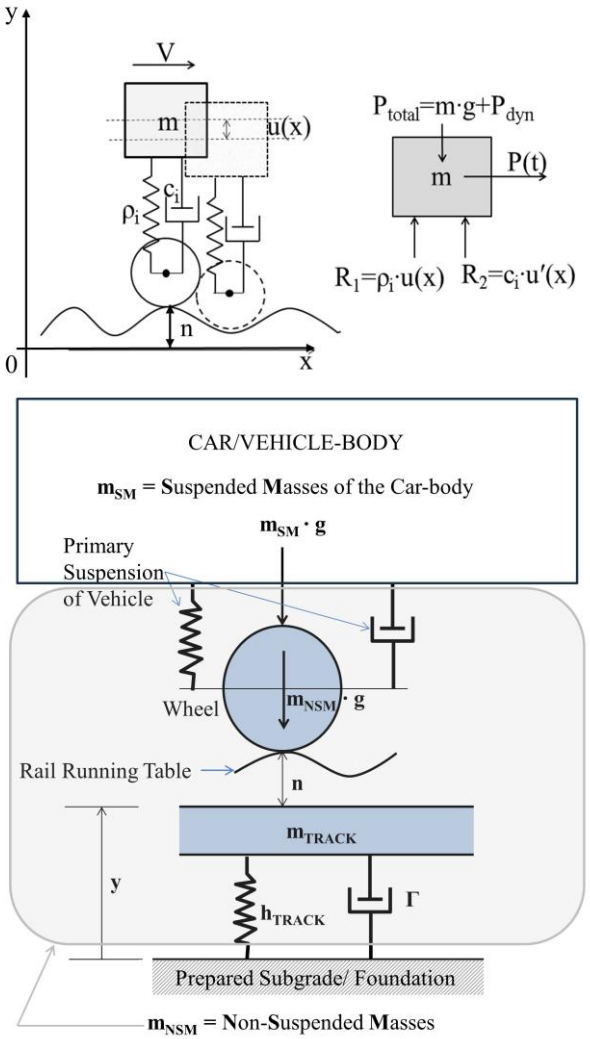

Figure 13. (Upper) The most simplified approach of this motion (vehicle on Track) is simulated by a SDOF [= Single Degree Of Freedom] system. (Lower) Schematic mapping of a vehicle/car on a Raiway Track: m_{NSM} the Non-Suspended Masses (under the primary suspension) of the vehicle (the not depicted secondary suspension is between the bogie-frame and the car-body); m_{TRACK} the mass of the track that participates in the motion of the Non-Suspended Masses (m_{NSM}); m_{SM} the Suspended Masses of the vehicle/car-body (above the primary suspension); Γ damping constant of the track; h_{TRACK} the total dynamic stiffness coefficient of the track; n the fault ordinate of the Rail Running Table, and y the deflection of the track. The dynamic component is owed to the NSM and the SM [see [21]].

$$\Rightarrow Q_\alpha = \frac{2 \cdot \alpha \cdot h_{CG}}{e^2} \cdot Q_{wheel} \qquad (10.1)$$

This additional semi-static Load is distributed to the adjacent sleepers as also the $Q_{\text{wheel-static}}$.

Now we have to calculate the dynamic overloads [or dynamic component of the acting total Load on Track] -namely the reaction per support point of the rail, $R_{dynamic}$-, due to the dynamic actions; the $R_{dynamic}$ should be added to the previous $R_{static/semi-static}$.

These dynamic overloads can be separated into three distinct fractions according to the frequencies involved:

1.-Dynamic Overloads in the frequency band 0,5 to 15 Hz

These are primarily due to the movements and reactions of the vehicles' Suspended Masses, which are excited, at commonly used speeds, by Track defects measured by the Recording Cars in the wavelength band 3-50 m [see [30]].

These low frequencies correspond to the inherent movements of the vehicle-body and bogie suspensions: 0,5 to 3 Hz for the body suspensions, and 5 to 10 Hz for the movements of the intermediate Suspended Masses of the bogies. The coupling between these different stages prevents their separation.

To summarize, it should be noted that the various measurements carried out on board the High Speed trains, in a speed range of 50-300 km/h, showed that these overloads can be considered, for the type of modern suspension equipping the trains, as increasing linearly with speed, their standard deviation being practically proportional, at a given speed, to the standard deviation of the longitudinal vertical defects as it can be calculated from the recordings.

In order to reduce these overloads, it is much easier to intervene at the level of the suspension characteristics of the vehicles than on the geometric quality of the Track.

2.-Dynamic Overloads in the frequency band 20 to 200 Hz

These forces are caused by the movements of Non-Suspended (Unsprung) Masses which are attached to a piece of Track Mass along the trajectory of the wheel [10]. They were initially studied as a simple, single-stage rheological model with a spring and viscous damper (Fig. 13). It should be noted that this model was subsequently developed, still as a simple rheological model, by adding stages to account for the properties of the different track components: rails, fastening-pads, sleepers, ballast, and substructure (see Fig. 4). These models, despite their obvious limitations -since they cannot account for the continuous movement of the wheel-mass on the rail- allow us to understand the influence of various track parameters and the statistical evolution of the loads due to Non-Suspended Masses with speed. The differential Eqn of motion is given by:

$$\left(m_{NSM}+m_{TRACK}\right)\cdot\frac{d^2y}{dt^2}+\Gamma\cdot\frac{dy}{dt}+h_{TRACK}\cdot y=$$

$$=-m_{NSM}\cdot\frac{d^2n}{dt^2}+\left(m_{NSM}+m_{SM}\right)\cdot g \qquad (10.2)$$

where: m_{NSM} depicts the Non-Suspended (Unsprung) Masses of the vehicle; m_{TRACK} is the mass of the track that participates in the motion; m_{SM} depicts the Suspended (Sprung) Masses of the vehicle that are cited above the primary suspension of the vehicle; Γ is the damping constant of the track (for its calculation see [11], [12]); n is the fault ordinate of the rail running table and y the total deflection of the track; h_{TRACK} is the total dynamic stiffness coefficient of the track (also $\rho_{dynamic}$), given by the equation (3.5) above:

$$h_{TRACK}=\rho_{total-dynamic}=2\sqrt{2}\cdot\sqrt[4]{E\cdot J\cdot\frac{\rho_{total\text{-}(static)}}{\ell}} \qquad (3.5)$$

If we are not interested but only for the Dynamic Overload, we can avoid the static terms since they represent the movement of the wheel around its equilibrium position, posing the auxiliary variables:

$$y_1=\left(\frac{m_{NSM}+m_{TRACK}}{h_{TRACK}}\right)\cdot g,\quad z=y+n-y_1$$

We also consider the mass (m_{TRACK}) of the Track participating in the motion of the NSM as negligible (or embodied in the NSM of the vehicle, since it is approximately 0,2 tonnes-mass) and the differential equation of motion (5.2) is transformed to:

$$m\frac{d^2z}{dt^2}+\Gamma\cdot\frac{d\left(z-n\right)}{dt}+h_{TRACK}\cdot\left(z-n\right)=0 \qquad (10.3)$$

Where z is the trajectory of the wheel, i.e. the leveling defect. The dynamic overload which is exerted by the wheel on the rail is:

$$\Delta Q=m\cdot\frac{d^2z}{dt^2}$$

namely, the NSM-mass multiplied by the vertical acceleration. The overload can be easily expressed taking the Fourier Transormations (F.T.) of the above terms, in relation to the defect(s) of Track:

if Z is the F.T. of z, $p=2i\pi\nu=i\omega$ variable of frequency, and N is the F.T. of n, then we have:

$$Eqn(5.3)\Rightarrow Z\cdot\left(mp^2+\Gamma\cdot p+h_{TRACK}\right)=$$

$$=\left(\Gamma\cdot p+h_{TRACK}\right)\cdot N$$

or

$$\frac{Z}{N}=\frac{h_{TRACK}+\Gamma\cdot p}{m\cdot p^2+\Gamma\cdot p+h_{TRACK}} \qquad (10.4)$$

Eqn (10.4) characterizes the Transfer Function between the trajectory of the wheel and the defect of the Track and permits to calculate the Transfer Function between the Dynamic Overload and the defect:

$$\frac{\mathbb{F}(\Delta Q)}{N}=\frac{m\cdot p^2\cdot\left(h_{TRACK}+\Gamma\cdot p\right)}{m\cdot p^2+\Gamma\cdot p+h_{TRACK}}=H(\omega) \qquad (10.5).$$

Where $\mathbb{F}$ = F.T. = Fourier Transform. H(ω) is a complex function. However, interesting results can be derived from the equations which relate the Spectral Densities of the Input and the Output of a system (e.g. wheel – defects, excitation – response) [[10], [21], [22]]. If $S_{\Delta Q}$ and S_n are the Spectral Densities of Energy of the Dynamic overload and of the defect of the Track:

$$S_{\Delta Q}(\omega)=\left|H(\omega)\right|^2\cdot S_n(\omega) \qquad (10.6)$$

and the Variance (for SM see [15]):

$$\sigma^2(\Delta Q)=\frac{1}{\pi}\cdot\int_0^\infty S_{\Delta Q}\cdot d\omega,\quad \sigma^2(n)=\frac{1}{\pi}\cdot\int_0^\infty S_n\cdot d\omega \qquad (10.7)$$

The relation between the Excitation Spectrum of time-space domain and the frequencies domain is:

$$\int_0^\infty S(\omega)\cdot d\omega=\int_0^\infty S(\Omega)\cdot d\Omega,\quad \omega=V\cdot\Omega \qquad (10.8)$$

where ω is the pulsation in time-space domain, Ω is the pulsation in frequencies domain and V the circulation speed of the vehicle.

The representative equation of the Spectral Density of short wavelengths is [18]:

$$S_n(\Omega)=\frac{A}{(B+\Omega)^3} \qquad (10.9)$$

Fron Eqn (10.8) we derive (after some mathematical calculations see [18]) that:

$$\sigma^2(\Delta Q_{NSM})=m_{NSM}^2\cdot\sigma^2(\gamma)=\left(\underbrace{1{,}3433\cdot A}_{k_a^2}\right)\cdot V^2\cdot m_{NSM}\cdot h_{TRACK}=$$
$$=\underbrace{\sqrt{1{,}3433\cdot A}}_{k_a}\cdot V\cdot\sqrt{m_{NSM}\cdot h_{TRACK}}\Rightarrow$$
$$\Rightarrow\sigma^2(\Delta Q_{NSM})=k_a\cdot V\cdot\sqrt{m_{NSM}\cdot h_{TRACK}} \qquad (10.10)$$

The linear increase of the dynamic overloads due to the NSM in relation to the speed which results from the Excitation Spectrum, has been verified by the measurements performed by the train TGV of tests on the Track for speeds between 50 and 300 km/h [[9], [8]].

3.-Dynamic Overloads in the frequency band 200 to 2000 Hz

These overloads are owed to the contact wheel-rail, and the constitutive elements of the system that are part of this contact: wheel, rail, fastenings. This contact provokes the "undulatory wear" of the Rail Running Table, which has been mentioned above.

11 Statistical Analysis of Spectra of the Track Recordings

The mean square value of the defects z is expressed as a function of their power spectral density in space:

$$\sigma^2(z)=\frac{1}{\pi}\cdot\int_0^\infty S_z(\Omega)\cdot d\Omega \qquad (11.1)$$

In real conditions, since on the Track section a vehicle circulates with a speed V, the excitation is represented by a function in the time-space domain after a change of variable $x=V\cdot t$.

We name as:

S(Ω) the spectrum in the time-space domain and,

s(ω) the spectrum in the frequencies' domain.

The mean square value of the amplitudes of the defects $\sigma^2(z)$ is independent of the variable and *the Eqn (10.8) is valid*.

We can transform the equation for the mean square value, if we normalize the spectrum of defects in a form of the type (see Eqns 6.4.15, 4.4, 4.5):

$$S_z(\Omega)=\pi\cdot\sigma^2(z)\cdot\Phi_z(\Omega) \qquad (11.2a)$$

And the spectrum of the excitation (the movement of the vehicle) in a form:

$$S_z(\omega)=\pi\cdot\sigma^2(z)\cdot\varphi_z(\Omega) \qquad (11.2b)$$

With:

$$\varphi_z(\omega)=\frac{1}{V}\cdot\Phi_z\left(\frac{\omega}{V}\right) \qquad (11.2c)$$

Consequently:

$$\int_0^\infty\Phi_z(\Omega)\cdot d\Omega=\int_0^\infty\varphi_z(\omega)\cdot d\omega=1 \qquad (11.3)$$

In a real Track section, after executing works of longitudinal leveling, the amplitudes of the defects which correspond to wavelengths from some meters to some decades of meters ameliorate due to these works of maintenance. The graph spectrum of defects -after the works of maintenance- is moved in parallel position of the praph before the works. If this new graph is characterized by a function $\Phi_{after}(\Omega)$, satisfying also an Eqn of the same form:

$$S_z(\Omega) = \pi \cdot \sigma^2(z') \cdot \Phi_z(\Omega) \qquad (11.2.a_1),$$

then the functions $S(\Omega)$ and σ_2 of the new graph of the spectral density of the defects are enough to evaluate the evolution of the Track quality.

The function $\Phi(\Omega)$ is dependent on the materials which constitute the Track-panel (rails, sleepers, fastenings etc.) on the age of the Track and the nature of the foundation of the Track.

Function S is -finally- well represented by:

$$S(\Omega) = \frac{\mu}{\left(1 + \frac{\Omega}{\lambda}\right)^n} \qquad (11.4)$$

with the 3 parameters λ, μ, n being enough to characterize the spectrum, where μ is parameter of amplitude of the defect, and n ≈3 always.

In reality, for each Track-section, we know the constitutive elements of the track and of the vehicle as well, thus, the coefficients in Eqn (11.4) become a constant and we derive the following Eqn:

$$\sigma^2(\Delta Q) = k \cdot \sigma^2(z) \qquad (11.5)$$

which is the relation between the variance of the dynamic overload to the variance of the defects of Track (Eqn 10.10 and Eqns 10.4, 10.6, 10.7, 10.8).

$$Eqn(10.5) \Rightarrow \mathbb{F}(\Delta Q) = \mathbb{F}(n) \cdot H(\omega) \qquad (10.5a)$$

Where $\mathbb{F}$ = the Fourier Transform.

In the theory of stochastic systems, the spectra are linked to Fourier Transforms ($\mathbb{F}$= F.T.). For deterministic systems the spectra and the Fourier Transformation are used to represent a function as superposition of exponential functions. For random systems (or signals) the concept of spectrum has two interpretations. The first one includes transforms of averages and is essentially deterministic. The second one includes the representation of the process as a superposition of exponential functions with random coefficients. The *Power Spectrum* or *Spectral Density* of a stochastic system -that is described by a function *x(t)*- is the Fourier Transform of the system's auto-correlation function $\Phi_x(t)$ [[28] 10-3: Power Spectrum]:

In general, if we begin our analysis from periodic excitations, with period T, and passing to the case that $T \to \infty$, then the derived Force as response with $\omega_0 \to d\omega$ and $\nu\omega_0 \to \omega$:

$$F_i(t) = \int_{-\infty}^{+\infty} \frac{1}{2\pi} \cdot \int_{-\infty}^{+\infty} \left(F_i(t) \cdot e^{-i\omega t} \cdot dt\right) \cdot e^{i\omega t} \cdot d\omega \quad (11.6)$$

where, ***we define(d) as the frequency Spectrum of excitation*** (or response since the subsidence or the defect of the track and the resultant force are excitation or response to each other), the relation:

$$f_i(\omega) = S(\omega) = \frac{1}{2\pi} \cdot \int_{-\infty}^{+\infty} F_i(t) \cdot e^{-i\omega t} \cdot dt \qquad (11.7)$$

as it is described analytically in [[10], ch. 3, **120-121**].

The excitation (rail irregularities/track defects) in reality is random and neither periodic nor analytically defined. It can be defined by its autocorrelation function in space and its spectral density. If *f(x)* is a signal with determined total energy and *F(v)* its Fourier transform, from Parseval's modulus theorem, the total energy of the signal is [18]:

$$\int_{-\infty}^{+\infty} |f(x)|^2 \cdot dx = \int_{-\infty}^{+\infty} |F(\nu)|^2 \cdot d\nu \qquad (11.8a)$$

where, $F(v) = A(v) \cdot e^{i\varphi(v)}$ and the power spectral density:

$$S(\omega) = |F(\nu)|^2 = A^2(\nu) \qquad (11.9)$$

Reference [31] solves Eqn. (11.8a) as:

$$\int_{-\infty}^{+\infty} f(t)^2 \cdot dt = \frac{1}{2\pi} \int_{-\infty}^{+\infty} F(\omega)^2 \cdot d\omega \qquad (11.8b)$$

The square of the modulus $F(\omega)$ is called the energy spectrum of the signal because $F^2(\omega) \cdot \Delta(\omega)$ represents the amount of energy in any $\Delta\Omega$ segment of the frequency spectrum and the integral of $F^2(\omega)$ over $(-\infty, +\infty)$ gives the total energy of the signal.

An input signal -like the running rail table- creates through the vehicle an output signal: the wheel trajectory. The output spectral density and the input spectral density of the excitation are related through equation [18]:

$$S_{out}(\bar{\omega}) = |H(i\bar{\omega})|^2 \cdot S_{in}(\bar{\omega}) \qquad (11.9a)$$

To relate the frequency spectrum with the spectrum in space we use the following equation:

$$\omega \cdot t = \frac{2\pi V t}{\lambda} \Rightarrow \omega = \frac{2\pi}{\lambda} \cdot V \Rightarrow \omega = \Omega \cdot V \qquad (11.9b)$$

where λ is the wavelength of the defect. This means that the circular frequency in space Ω is the wave number k of the equation of oscillation, and applying a property of the Fourier transform [18]:

$$\int_0^{\infty} S(\Omega)\cdot d\Omega = \int_0^{\infty} s(\omega)\cdot d\omega \Rightarrow \mathbb{F}\left[f(ax)\right] = \frac{1}{|a|}\cdot \hat{f}\left(\frac{\nu}{a}\right) \Rightarrow$$

$$S(\omega) = S\left(\frac{\Omega}{V}\right) = \frac{1}{V}\cdot S(\Omega) \qquad (11.10)$$

where $\mathbb{F}$ = Fourier Transform of f and $\hat{f}$ is the function after the Fourier Transform. The Variance or mean square value $\sigma^2(x)$ of the function is given by:

$$\sigma^2(x) = \frac{1}{2\pi}\cdot \int_{-\infty}^{+\infty} S(\omega)\cdot d\omega = \bar{x}^2 \qquad (11.11)$$

and the standard deviation is

$$\sigma(x) = \sqrt{\sigma^2(x)}$$

From (11.11) we derive [18]:

$$\sigma^2(n) = \frac{1}{\pi}\int_0^{+\infty} S_n(\omega)\cdot d\omega, \qquad (11.12a)$$

$$\sigma^2(z) = \frac{1}{\pi}\int_0^{+\infty} S_z(\omega)\cdot d\omega, \qquad (11.12b)$$

$$\sigma^2(\Delta Q) = \frac{1}{\pi}\int_0^{+\infty} S_{\Delta Q}(\omega)\cdot d\omega \qquad (11.12c)$$

where *n* is the random variable of the defect (input), *z* the subsidence of the wheel (output) and *ΔQ* the dynamic component (overload) of the acting total Load due to the Non-Suspended Masses (at this point the relevant dynamic component due to the SM is omitted), that is added to the Static and Semi-static Components of the Load of the wheel (output also) [18].

From these equations and the analytic form of the spectrum of the defects/faults, we can calculate the mean square value of the dynamic component of the Load due to the Non Suspended Masses $\sigma(\Delta Q_{NSM})$, as in Eqns (10.7), (10.10).

From the power spectral density and the variance functions and their definitions ([10], [18]):

$$S_{\Delta Q}(\omega) = S_n(\omega)\cdot\left|B(\omega)\right|^2 \qquad (11.13)$$

which coincides with Eqn. (11.5) above.

The utilization of the Spectral Density of the defects of the Track, as it results from the recordings of the Tack-defects, gives a full image of the existing Track geometry at any moment and the factors that should be ameliorated for better function of the Track too. Thus we are able to make decisions for the correct maintenance, in order to achieve a better quality in the circulation of the trains at each Track section.

12 Accuracy of the Estimation of the Spectral Density of the Recording(s) of the Track

As it has been presented ([21], [22]), the (Power) Spectral Density of a random signal (e.g. the recording of the measurement(s) of the defects of a Railway Track) at a point x_0 at the space-time domain (Fig. 3) includes the entire history (the future is included also) of *f(x, t)* for what corresponds to each frequency v_i. According to Fourier's Theory any arbitrary (random) function, even one with a finite number of discontinuities, could be represented as (decomposed to) an *infinite summation of sine and cosine terms*. Furthermore, the Spectral Density has the important property that ***an approximation consisting of a given number of terms achieves*** (since, after a number of few terms, the next terms do not contribute significantly) ***the minimum mean square error between the (real) signal and the approximation***. Consequently, since we can measure the (Power) Spectral Density of the output -*that is of the recording of the measured values by the Track Recording Vehicle*-, then the (Power) Spectral Density of the input -*that is of the real (vertical) defects of the Track*- can be accurately calculated from the output Spectral Density and the Recording Vehicle's Transfer Function *K(Ω)*; *K(Ω)* is well, mathematically, defined for every Car/Vehicle (see [21], [22]). Hence, *there is not any problem of accuracy in the calculation of the Spectral Density of the output (recorded measurements) and from that of the calculated value of the Spectral Density of the real Track's Defects*.

However, the following issue has been arised, in general: "the essence of the spectral estimation problem is captured by the following informal formulation: *from a **finite record** of a stationary data sequence, estimate how the total power is distributed over frequency*".

Yet, the Recordings of the Measurements of a Track Section (e.g. Domokos-Larissa in Greece) are performed by the Track Recording Car *all over the whole length of this Track Section* and not to a part of its length, namely, it is not a sample (partial in length) recording. The *critical remark on this case* -based on the reality in Railways- is: the recordings of the measurements are performed *all over the whole length of a Track Section* -from which recordings, we derive the spectral density of this Track Section- and not to a "*single finite segment of the 'signal'*" ["="Track Section's defects"]. Only in the latter case an "aliasing issue" could have been introduced, and not in the real case of the measurements of a Railway Track [22].

11 Synopsis - Conclusions

In this article, which is a continuation of [21] and [22], real Recordings from Track sections with the graphs of the Spectral Densities which are derived from these recordings were presented. Furthermore, they were presented: the Dynamic Vertical Stresses on the Trackbed due to the Excitation Spectra of the Track, the Response of the "Track-Vehicle system" to the Track defects in relation to their Spectral Density, a Statistical Analysis of Spectra of the Track Recordings, as well as the utilization of Spectra to make correct decisions for the Track maintenance works.

The basic data of this article resulted from theoretical and experimental investigation during the cooperation between experts of OSE and SNCF (1988-1989) and personal research of the author either in the Hellenic Railways Organization (OSE) or at the University of Thessaly, Civil Engineering Department (2007-2014) but also later until now (2025).

Acknowledgement

I want to specially thank professor T.P. Tassios for his questions and suggestions, after the publication of [22], which led me to investigate the issue presented here. In any case, any existing mistakes in the present article are exclusively mine.

References

[1]. Alias, J. 1984. *La Voie Ferree – Techniques de Construction et Entretien*, deuxieme edition, Eyrolles, Paris.

[2]. Argyris, J., and, P.-H., Mlejnek. 1991. *Dynamics of Structures*, Elsevier Science Publishers B.V.

[3]. Clough, R.W., and, J., Penzien. 1993. *Dynamics of Structures*, second edition, McGraw-Hill Intl., Singapore.

[4]. Cope, G.H. 1993. Completely Rewritten. *British Railway Track – Design, Construction and Maintenance*, publ. by the Permanent Way Institution, Loughborough, Leicester, England, 1943.

[5]. Eisenmann J., Duwe B., Lempe U., Leykauf G., Steinbeisser L. 1979. Entwicklung, Bemessung und Erforschung des schotterlosen Oberbaues "Rheda". AET (34), 23-41.

[6]. Fortin, J. 1982. La Deformee Dynamique de la Voie Ferree, RGCF, 02/1982.

[7]. Gent, I., and, G., Janin. La Qualite de la Voie Ferree, SNCF's reprint.

[8]. Giannakos, K., Domsa-Vlassopoulou, I., and, P., Iordanidis. 1988. *Έκθεση Επιτροπής Εμπειρογνωμόνων του ΟΣΕ για την Επίσκεψη στους SNCF αρ;ο 15/5/1988-11/6/1988*, Αθήνα.

[9]. Giannakos, K., Domsa-Vlassopoulou, I., and, P., Iordanidis. 1989. *Πρακτικά Συναντήσεων κατά τη Συνεργασία με τους SNCF στο Παρίσι-St Ouen*, Παρίσι/Αθήνα.

[10]. Giannakos, K. 2004. *Actions on the Railway Track*, Papazissis, Athens, Greece, translation from the Greek edition 2002.

[11]. Giannakos, K. 2010a. Loads on track, Ballast Fouling and Life-cycle under Dynamic Loading in Railways, *International Journal of Transportation Engineering – ASCE, Vol. 136, Issue 12*, 1075-1084.

[12]. Giannakos, K. 2010c. Interaction between Superstructure and Substructure in Railways. *Fifth International Conference on Recent Advances in Geotechnical Earthquake Engineering and Soil Dynamics and Symposium in honor of professor I. M. Idriss, San Diego, CA - USA, May 24-29 proceedings*.

[13]. Giannakos, K. 2010d. Theoretical calculation of the track-mass in the motion of unsprung masses in relation to track dynamic stiffness and damping, *International Journal of Pavement Engineering (IJPE) 11*, No.4, 319–330. Special Rail Issue High-Speed Railway Infrastructure: Recent Developments and Performance.

[14]. Giannakos, K. 2013a. Track Defects and the Dynamic Loads due to Non-Suspended Masses of Railway Vehicles, *International Journal of Mechanics, Vol. 7, Is. 3*, 180-191.

[15]. Giannakos, K. 2013b. *Second Order Differential Equation of Motion in Railways: the Variance of the Dynamic Component of Actions due to the Unsprung Masses*, AMCME 2013, The 2013 International Conference on Applied Mathematics and Computational Methods in Engineering, July 16-19, 2013, Rhodes (Rodos) Island, Greece, proceedings.

[16]. Giannakos, K. 2014. Actions on a Railway Track, due to an Isolated Defect,

International Journal of Control and Automation Vol.7, No.3, 195-212.

[17]. Giannakos, K. 2016a. Deflection of a railway reinforced concrete slab track: Comparing the theoretical results with experimental measurements, *Engineering Structures Journal (122)*, Elsevier, 296-309.

[18]. Giannakos, K. 2016b. Modeling the Influence of Short Wavelength Defects in a Railway Track on the Dynamic Behavior of the Non-Suspended Masses, *Journal Mechanical Systems and Signal Processes (jmssp), Elsevier,* 68-83, http://dx.doi.org/10.1016/j.ymssp.2015.07 . 020.

[19]. Giannakos, K. 2022. Control of the Geometry of a Railway Track: Measurements of Defects and Theoretical Simulation, International Journal on Applied Physics and Engineering, Vol.1, 102-115, https://wseas.com/journals/ape/2022/a22ape011(2022).pdf.

[20]. Giannakos, K. 2023. Influence of Track Defects on the Track-Loads and Confidence Interval of a Track Recording Car, *WSEAS Transactions on Applied and Theoretical Mechanics,* Vol. 18, 2023, 16-31, https://wseas.com/journals/mechanics/2023-a065111-001(2023).pdf.

[21]. Giannakos, K. 2024. Railway System 'Vehicle-Track': Relation Between the Spectral Density of Excitation vs of Response, *International Journal of Mechanical Engineering*, Vol.9, 1-14. https://www.iaras.org/home/caijme/railway-system-vehicle-track-relation-between-the-spectral-density-of-excitation-vs-of-response.

[22]. Giannakos, K. 2025. Railway System 'Vehicle-Track': Simulation, Mathematical Modelling and Spectral Densities of Excitation and Response (Part II), *International Journal of Mechanical Engineering, Vol. 10, 56-74*. https://www.iaras.org/home/caijme/railway-system-vehicle-track-simulation-mathematical-modelling-and-spectral-densities-of-excitation-and-response-part-ii.

[23]. Marple, S.L., Jr. 2019/1987. 2nd Edition. *Digital Spectral Analysis*, Dover publ., Mineola, NY.

[24]. Max, J. 1985. *Methodes et Techniques de Applications aux Mesures Physiques*, Masson, Paris.

[25]. OSE/SNCF Cooperation. 1988. *Comportement des Traverses en relation avec les Charges Dynamiques*, *Report 1*, Juin 1988.

[26]. OSE/SNCF Cooperation. 1989. *Programme d' essais realize au centre d' essais de la Direction de l' Equipement Report 2*, 3/1989.

[27]. Papoulis, A. 1962. *The Fourier Integral and its Applications*, Mc Graw Hill, 1962, series classic textbooks.

[28]. Papoulis, A. 1991. *Probability, Random Variables and Stochastic Processes*, third edition, McGraw-Hill Intl., Singapore.

[29]. Roddier F. 1971. *Distributions et Transformation de Fourier*, Edisciense, Paris.

[30]. SNCF/Direction de l' Equipement. 1981. *Mecanique de la Voie*, Paris.

[31]. Wylie, C.R., and, L.C. Barrett. 1995. *Advanced Engineering Mathematics*, sixth edition, McGraw-Hill, Inc., USA.